research articles Journal of proteome research

# A Comparative Study of Electrostatic Repulsion-Hydrophilic Interaction Chromatography (ERLIC) versus SCX-IMAC-Based Methods for Phosphopeptide Isolation/Enrichment

**Chee Sian Gan,[†] Tiannan Guo,[†,‡] Huoming Zhang,[†] Sai Kiang Lim,[§] and Siu Kwan Sze*[,†]**

*School of Biological Sciences, Nanyang Technological University, 60 Nanyang Drive, Singapore 637551, Singapore, Division of Medical Sciences, National Cancer Centre Singapore, 11 Hospital Drive, Singapore 169610, Singapore, and Institute of Medical Biology, 8A Biomedical Grove, #05-505 Immunos, Singapore 138648, Singapore*

**Received June 27, 2008**

Electrostatic repulsion-hydrophilic interaction chromatography (ERLIC) has been introduced recently for phosphopeptide enrichment. Here we compared ERLIC with the well-established SCX-IMAC for identifying phosphopeptides in EGF-treated A431 cells. The ERLIC approach detected a higher number of phosphopeptides (17 311) than SCX-IMAC (4850), but it only detected 926 unique phosphopeptides compared to 1315 in SCX-IMAC. Only 12% unique phosphopeptides were common to both approaches, suggesting that more comprehensive phosphoproteomes could be generated by complementing SCX-IMAC with ERLIC.

**Keywords:** Phosphopeptide enrichment • EGFR signaling • A431 carcinoma cells • WAX • IMAC • ERLIC • SCX

## Introduction

Protein phosphorylation is one of the most important reversible post-translational modifications and it is critical in many aspects of cellular functions such as signal transduction. Its importance is underlined by the fact that, in mammalian cells, at least one-third of all proteins are phosphorylated.[1] Therefore mapping the phosphoproteome and the dynamic changes in phosphoproteomic profile of cells in different physiological states will facilitate a better understanding of protein phosphorylation and their molecular functions in different aspects of cell biology. Consequently, much effort has been spent building universal phospho-databases, for example, NetworKIN,[2] Human Protein Reference Database,[3] PHOSIDA,[4] and PhosphoSitePlus (http://www.phosphosite.org).

However, most phosphorylated proteins are not only low in abundance, their relative concentrations also change rapidly in response to changes in their physiological states and cellular activities. Therefore, some of the major challenges in phosphoproteome mapping are low phosphorylation stoichiometry and phosphopeptide copy number.[5] To overcome these challenges, it is necessary to develop methods to enrich phosphorylated proteins/peptides.

Methods for enrichment of phosphorylated proteins are often optimized using the epidermal growth factor receptor (EGFR) signaling pathway as a model system. It is a well-characterized biological process that is modulated by phosphorylation[6] and at least 14% of all phosphorylation sites are known to be regulated by EGF.[7] Additionally, phosphorylation events in EGFR signaling are associated with cancer in humans.[8]

Many methods for phosphopeptide enrichment have been described and these include phosphoramidate chemistry (PAC),[9] phospho-specific antibodies immunoprecipitation,[10] immobilized metal affinity chromatography (IMAC),[11] strong-cation exchange (SCX) chromatography,[12] and titanium dioxide ($TiO_2$) chromatography.[13] One of the more robust methods uses a combination approach of SCX chromatography followed by IMAC affinity purification.[14] Using this approach, Villén et al. identified more than 5600 nonredundant phosphorylation sites on 2300 proteins in mouse liver.[14] Another similar method couples SCX with $TiO_2$ chromatography. Here, 6600 phosphorylation sites on 2200 HeLa cell proteins were detected.[7] The $TiO_2$ and the IMAC methods were found to be complementary[15] and using the combination of the two methods generated a larger and enhanced set of information that surpasses the outcome derived using one method.[14,16,17]

ERLIC (Electrostatic repulsion-hydrophilic interaction chromatography) has been introduced recently as a potential phosphopeptide enrichment method.[18] Unlike the SCX-IMAC approach, this approach achieves both sufficient phosphopeptide enrichment and fractionation in a single step. It is based on hydrophilic interaction and electrostatic repulsion. At low pH (such as pH 2), carboxyl group at Asp- and Glu-residues and the C-terminus are largely un-ionized such that during weak anion exchange (WAX) chromatography, peptides are generally electrostatically repulsed by the column at their positively charged N-termini. However, a phosphopeptide with its negatively charged phosphate group will be electrostatically attracted to WAX and this interaction increases column reten-

* To whom correspondence should be addressed. Dr. Siu Kwan Sze, tel, (+65)6514-1006; fax, (+65)6791-3856; e-mail, sksze@ntu.edu.sg.
[†] Nanyang Technological University.
[‡] National Cancer Centre Singapore.
[§] Institute of Medical Biology.

10.1021/pr800473j CCC: $40.75 

Published on Web 10/02/2008

tion time of phosphopeptides compared with nonphosphopeptides. Column retention is further enhanced by the use of high concentration of organic solvent (such as 70% acetonitrile) which promotes hydrophilic interaction of the phosphate group with the column.[18] A salt gradient is then used to elute phosphopeptides from the column. Although it has been claimed that this ERLIC approach of using WAX chromatography in the presence of low pH, high organic solvent content, and salt gradient could enrich phosphopeptides from the nonphosphopeptides,[18] there has been no direct comparison between ERLIC and established methods like SCX-IMAC to determine the relative efficiency of the ERLIC approach.

In this comparison, we also included SCX via early elution[12] as the enrichment of phosphopeptides by SCX and WAX or ERLIC is based on diametrically opposite parameters of electrostatic repulsion or attraction, respectively. Therefore, these two phosphopeptide enrichment methods could potentially complement each other in phosphopeptide enrichment particularly if they enrich for different sets of phosphopeptides. In this study, we compared the phosphoproteome of EGF-treated A431 cells determined using ERLIC, SCX-IMAC, and SCX-only approaches. The efficiency of the workflow, phosphopeptide enrichment, the number of phosphopeptides, and phosphorylation sites detected, as well as the number of unique phosphorylated proteins detected by both approaches, were then compared. This study demonstrated that the ERLIC approach could potentially complement the SCX-IMAC approach to generate a more complete phosphoproteome.

## Materials and Methods

**Sample Preparation.** The human epithelial carcinoma cell line A431 was obtained from ATCC. Cells were cultured at 37 °C in a 5% $CO_2$-air atmosphere in DMEM supplemented with 10% fetal bovine serum (Hyclone, Thermo Fisher Scientific, Inc., Waltham, MA), 100 U of penicillin, and 100 $\mu$g of streptomycin per mL (Invitrogen, Carlsbad, CA). To stimulate phosphorylation, cells were first serum-starved for 16 h, and then treated with 50 ng/mL EGF (Becton, Dickinson and Company, Franklin Lakes, NJ) for 10 min before being homogenized by douncing in a buffer consisting of 50 mM HEPES (pH 7.5), 8 M urea, 75 mM NaCl, a mixture of phosphatase inhibitor cocktail (PhosSTOP, Roche Applied Science, Indianapolis, IN) and protease inhibitor cocktail (COMPLETE, Roche Applied Science). Protein sample was reduced with 10 mM DTT for 1 h at 37 °C, then alkylated with 55 mM Iodoacetamide for 30 min at room temperature, before being digested with trypsin in a 1:50 (trypsin/protein) mass ratio. Prior to tryptic digestion, the protein sample was diluted 8 times with 50 mM HEPES (pH 7.5) to approximately 1 M urea. The protein concentration was measured using bicinchoninic acid (BCA) assay. All chemicals were purchased from Sigma-Aldrich (St Louis, MA) unless otherwise stated.

**SCX Workflow.** A total of 10 mg of peptide was fractionated using a PolySULFOETHYL A column (4.6 mm × 100 mm, 5 $\mu$m particle size, 200 Å pore size) (PolyLC, Columbia, MD) on a Shimadzu Prominence UFLC system (Kyoto, Japan). To prevent column overloading, 10 mg of peptide was separated into 4 different runs with each run of approximately 2.5 mg. A 60 min shallow gradient designated for phosphopeptides separation using a combination of 5 mM $KH_2PO_4$ in 30% acetonitrile, pH 2.65 (Buffer A) and Buffer A with 350 mM KCl, pH 2.65 (Buffer B) was created.[14] The gradient was composed of 100% A for 5 min; then 0−21% B for 35 min; followed by 21−100% B for 5 min; then maintained at 100% B for 10 min; finally ending at 100% A for 5 min. The column was conditioned in 100% A for 30 min after each gradient and before the next run to ensure reproducibility. The UV detection was monitored at a wavelength of 214 nm. A total of 24 fractions (out of 55 fractions) were collected by pooling most fractions at 2 min intervals and a few (beginning and ending fractions) at 3 min intervals.

Identical fraction numbers from each run were combined, dried via lyophilization, and desalted using SEP-PAK C18 cartridges (Waters Corporation, Milford, MA).

**IMAC Enrichment.** Each SCX fraction was dissolved in 100 $\mu$L of Wash buffer (250 mM acetic acid with 30% acetonitrile, pH 2.60), and subsequently added to 20 $\mu$L of IMAC slurry (50% gel) (Phos-Select, Sigma-Aldrich) for 1 h at room temperature with end-over-end rotation. The IMAC slurry/gel was previously washed three times in Wash buffer. Phosphopeptides were eluted using 100 $\mu$L of 200 mM $Na_3PO_4$ (pH 8.4) by incubating at room temperature for 5 min. Elution was repeated twice using 100 $\mu$L each of 50 mM Tris (pH 10) and 400 mM $NH_4OH$ (pH 11). The eluate was immediately pH-adjusted to pH 2.60 using 10% formic acid, then dried via vacuum concentrator and desalted using SEP-PAK C18 cartridges.

**ERLIC Workflow.** As with the SCX approach, 10 mg of peptide was separated into 4 different runs of 2.5 mg each. The ERLIC mode separation was performed using a PolyLC Poly-WAX LP column (4.6 × 200 mm, 5 $\mu$m particle size, 300 Å pore size) on a Shimadzu Prominence UFLC unit. The gradient was created using a combination of 10 mM sodium methylphosphonate (Na-$MePO_4$) with 70% acetonitrile, pH 2.0 (Solvent A) and 200 mM triethylamine phosphate (TEAP) with 60% acetonitrile, pH 2.0 (Solvent B). The 60 min-gradient was composed of first 10 min at 100% A; followed by a ramp from 0−100% B for 35 min, then maintained at 100% B for 10 min; before re-equilibrating the column with 100% A for 5 min. Between runs, the column was conditioned in 100% A for 60 min. The UV detection was monitored at a wavelength of 214 nm. In total, 24 fractions (out of 55 fractions) were collected by pooling most fractions at 2 min intervals and a few (beginning and ending fractions) at 3 min intervals. Identical fraction numbers from each run were combined, dried via lyophilization and desalted using SEP-PAK C18 cartridges.

**Mass Spectrometric Analysis.** The LTQ-FT ultra (Thermo Electron, Bremen, Germany) was coupled with an online Shimadzu UFLC systems utilizing nanospray ionization. Peptides were first enriched with a Zorbax 300SB C18 column (5 mm × 0.3 mm, Agilent Technologies, Santa Clara, CA) followed by elution into an integrated nanobore column (75 $\mu$m × 100 mm, New Objective, Woburn, MA) packed with C18 material (5 $\mu$m particle size, 300 Å pore size, Michrom BioResources, Inc.). Mobile phase A (0.1% formic acid) and mobile phase B (0.1% formic acid, 100% acetonitrile) were used to establish the 90-min gradient comprised of 3 min of 0−5% B, then 52 min of 5−30% B, followed by 12 min of 30−60% B; maintained at 80% B for 8 min, before re-equilibrating at 5% B for 15 min.

The MS was operated in the data dependent mode as described previously[19] with some modifications. Sample was injected into the MS with an electrospray potential of 1.8 kV without sheath and auxiliary gas flow, ion transfer tube temperature of 180 °C, and collision gas pressure of 0.85 mTorr. A full survey MS scan (350−2000 $m/z$ range) was acquired in the 7-T FT-ICR cell at a resolution of 100 000 and a maximum ion accumulation time of 1000 ms. Precursor ion charge state screening was activated. The linear ion trap was used to collect

peptides where 10 most intense ions were selected for collision-induced dissociation (CID) in $MS^2$, which were performed concurrently with a maximum ion accumulation time of 200 ms. A $MS^3$ scan was followed after each $MS^2$ scan when a neutral loss at 97.97 Da was detected. Dynamic exclusion was activated for this process, with a repeat count of 1 and exclusion duration of 30 s. For CID, the activation $Q$ was set at 0.25, isolation width ($m/z$) 2.0, activation time 30 ms, and normalized collision energy of 35%.

**Data Analysis.** The extract_msn (version 4.0) program found in Bioworks Browser 3.3 (Thermo Electron, Bremen, Germany) was used to extract tandem MS spectra in the dta format from the raw data of LTQ-FT ultra. These dta files were then converted into MASCOT generic file format using an in-house program. Intensity values and fragment ion $m/z$ ratios were not manipulated. This data was used to obtain protein identities by searching against the IPI human protein database[20] (version 3.34; 67 758 sequences) by means of an in-house MASCOT server (version 2.2.03) (Matrix Science, Boston, MA). To estimate the rate of false positives (FP), the search was performed with 'target' (forward IPI human sequences) and 'decoy' (reverse IPI human sequences) database as described elsewhere.[21] The search was limited to maximum 2 missed trypsin cleavages; #$^{13}$C of 2; mass tolerances of 10 ppm for peptide precursors; and 0.8 Da mass tolerance for fragment ions. Fixed modification was carbamidomethyl at Cys residue, whereas variable modifications were oxidation at Met residue, and phosphorylation at Ser, Thr or Tyr residues. Only proteins with a MOWSE score higher than 42, corresponding to $p < 0.05$ were considered significant. The peptide/protein list(s) obtained was either exported to Microsoft Excel and Access, or processed using in-house script, for further analysis.

**Motif Analysis.** Possible phosphorylation motifs within the data set were analyzed using Motif-X algorithm.[22] Peptide sequences were centered on each phosphorylation sites, and extended to 13 amino acids in length. To distinguish between phosphorylated and nonphosphorylated Ser, Thr, and Tyr, phosphorylated residues were denoted by lowercase letters, whereas nonphosphorylated residues were uppercase. The IPI human database was used as the background. The maximum number of occurrences was set to 20, and the significance threshold was set to $P < 10^{-6}$. pTyr was not subjected to motif analysis since it was underrepresented in our data set. Four groups of motif classes were defined based on the composition of the amino acid residues. They are acidophilic (D and E containing sequences), basophilic (R and K containing sequences), Proline-directed (P containing sequences) and others.[14] The extracted motifs were then compared to the Human Protein Reference Database[3] for the known kinase substrate motif.

**Protein Classification and Pathway Analysis.** Phosphorylated proteins identified in this study were categorized into their respective biological processes and molecular functions using PANTHER classification system.[23] For kinase−substrate relationship, NetworKIN was used to extract the corresponding substrates.[2] Cytoscape (version 2.4.1) was used for the construction of protein−protein interaction network.[24]

## Results and Discussion

**Experimental Design.** In this study, A431 cells stimulated with EGF were subjected to phosphopeptides enrichment methods of SCX-IMAC (a), SCX-only (b), or ERLIC (c) (Figure 1). SCX-IMAC is a well-established two-step approach of enriching phosphoproteins by coupling SCX chromatography with IMAC affinity purification.[14,16] ERLIC, on the other hand, is a relatively new approach of identifying phosphopeptides in a single-step approach[18] and its applicability has yet to be proven. Here, we compared the robustness of the ERLIC approach to the more established SCX-IMAC method. A431 cells were prepared in a single batch for better consistency. A peptide mixture (10 mg/group) was subjected to chromatographic separation using WAX and SCX columns, for each approach (Figure 1).

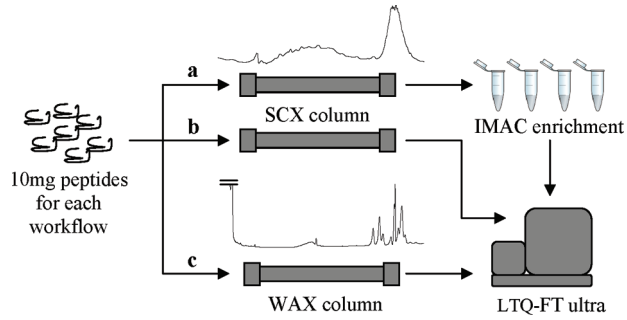


**Figure 1.** The overall schematic diagram of three different phosphopeptides enrichment strategies. (a) SCX-IMAC workflow, (b) SCX-only workflow, (c) ERLIC workflow. The chromatogram shown (UV detection at 214 nm wavelength) on top of each method/column was the general profile obtained through these approaches.

**$MS^3$-Dependent Verification.** A wide range of $MS^3$-independent and $MS^3$-dependent verification techniques are available to test the reliability of identified phosphopeptides.[7,25,26] $MS^3$-independent techniques utilizes the $MS^2$ spectrum to provide a scoring system based on the confidence level of the adjacent *b*- or *y*- ions next to the supposedly phosphorylated amino acid. Indeed many pSer and pThr phosphorylated peptides can be easily identified using $MS^2$ scan alone with high confidence without the need of $MS^3$.[27] $MS^3$-dependent technique uses an $MS^3$ scan to determine the reliability of the identified phosphopeptides.[15,25] $MS^3$ is triggered by the neutral loss from the previous $MS^2$ mass precursor and the likelihood that false phosphopeptides have matched to both $MS^2$ and $MS^3$ spectra is highly unlikely. Although $MS^3$ scan provides little information to the proper assignment of phosphorylation site,[26] it provides an added degree of confidence with minimal compromise as MS/MS scan rates are no longer rate limiting for high performance instrument such as LTQ-FT or LTQ-Orbitrap. Therefore, in this study, each $MS^2$ scan was followed by a subsequent $MS^3$ scan when a neutral loss was detected.

**Criteria for Phosphopeptides Identification.** When data generated using SCX-only, SCX-IMAC and ERLIC approaches were combined, a total of more than 22 000 phosphopeptides and 35 000 phosphorylation sites were identified (Table 1). The measured rate of false positive (FP) hits was less than 1% in all three approaches. To minimize the FP rate, we included only those peptides with MASCOT peptide score above 20. This is in line with Smith et al. describing significant amounts of FP hits below MASCOT peptide score of 17.[28] Furthermore, the MASCOT expectancy of peptide was also set to ≤0.05, except for those identified with $MS^3$ spectra (~20% of phosphopeptides).

As a whole, an average 75% of $MS^2$ spectra showed a neutral loss (i.e., $MS^3$) (Table 1), consistent with other observations that up to 79% of $MS^2$ spectra were accompanied by a neutral loss-

**Table 1.** Summary of the Protein/Peptide Identified in the Corresponding Workflows[a]

| | SCX-only | SCX-IMAC | ERLIC | All[#] |
|---|---|---|---|---|
| Total peptides (exp ≤ 0.05)* | 19880 | 6880 | 31036 | 57796 |
| Total decoys (exp ≤ 0.05)* | 181 | 21 | 154 | 356 |
| % False positives (FP)* | 0.91 | 0.31 | 0.50 | 0.62 |
| Total nonphosphopeptides | 19434 | 3195 | 15887 | 38516 |
| Unique nonphosphopeptides | 3076 | 873 | 925 | 3447 |
| Total nonphosphoproteins | 972 | 259 | 318 | - |
| Phosphopeptides (exp ≤ 0.05)* with $MS^3$ | 315 | 2446 | 10783 | 13545 |
| Phosphopeptides (exp > 0.05)* with $MS^3$ | 95 | 1167 | 2190 | 3452 |
| Phosphopeptides (exp ≤ 0.05)* without $MS^3$ | 231 | 1237 | 4338 | 5805 |
| Total phosphopeptides | 641 | 4850 | 17311 | 22802 |
| % Phosphopeptides enrichment | 3.21 | 60.27 | 52.10 | 37.23 |
| Total phosphopeptides with $MS^3$ | 410 | 3613 | 12973 | 16997 |
| % Phosphopeptides with $MS^3$ | 63.96 | 74.49 | 74.94 | 74.54 |
| Total unique phosphopeptides | 194 | 1315 | 926 | 2058 |
| Total phosphoproteins | 127 | 520 | 365 | 768 |
| Total phosphorylation sites | 766 | 8578 | 25915 | 35259 |
| Total unique phosphorylation sites | 202 | 984 | 761 | 1308 |
| No. of fractions | 24 | 24 | 24 | - |
| Workflow processing time | 1 day | 2 days | 1 day | - |
| MS instrument time[†] | 1.5 day | 1.5 day | 1.5 day | - |
| Total processing time | 2.5 days | 3.5 days | 2.5 days | - |

[a] Note that (*) 'exp' refers to MASCOT expectation value; whereas (#) 'All' refers to the combined statistic for all three approaches. (†) Average MS instrument time is 90 min × 24 samples = 1.5 day.

triggered $MS^3$ scan.[15] However, reduced ion statistics in $MS^3$ may hamper the percentage of $MS^2$−$MS^3$ matches. Therefore, to ensure that bona fide phosphopeptides were not excluded, those peptides that did not have $MS^3$ matches but did have a MASCOT peptide score of ≥20 and expectancy of ≤0.05 were included (Table 1). These phosphopeptides without $MS^3$ matches were also checked manually for correct assignment.

**Comparison of Phosphopeptide Enrichment Workflow.** Here we compare the efficiency of SCX-only, SCX-IMAC and ERLIC chromatographic separation workflow in enriching phosphopeptides for identification (Figure 1).

When peptides were separated into 24 fractions on SCX chromatography without any further phosphopeptide enrichment process such as IMAC, a total of 19 880 peptides were detected with a false positive (FP) rate of 0.91%. However, only 641 (3.2%) phosphopeptides were identified out of 1099 total proteins (Table 1). This indicates that SCX chromatography is mainly a fractionation method only. Although phosphopeptides are enriched and fractionated, significant amounts of nonphosphopeptides are coeluted.

When the peptides were enriched for phosphopeptide either by IMAC following SCX chromatography or the ERLIC method, there were significant increases in the number of phosphopeptides detected. The SCX-IMAC method identified 4850 of which 1315 were unique phosphopeptides, while the ERLIC method detected 17 311 phosphopeptides of which 926 were unique phosphopeptides (Table 1). Despite the much higher number of phosphopeptides (17 000) identified by the ERLIC method, the number of unique phosphopeptides identified was not correspondingly higher. Similarly, ERLIC uncovered 761 unique phosphorylation sites from an amazing total of 25 915 sites, while SCX-IMAC detected 984 unique phosphorylation sites from a total of 8578 total sites (Table 1); that is, one of every 9 sites identified by SCX-IMAC was unique, while only 3 of every 100 sites identified by ERLIC were unique. Therefore, SCX-IMAC approach outperformed ERLIC in enriching for a wider variety of phosphopeptides and this resulted in the detection of more unique phosphopeptides and phosphorylation sites with much reduced redundancy.

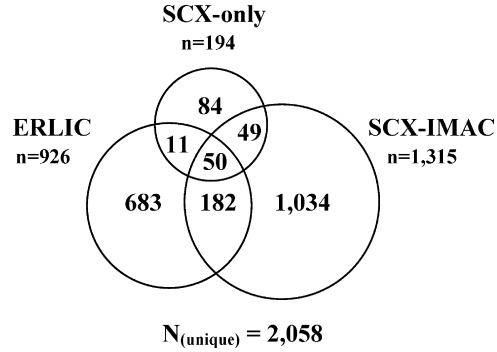


**Figure 2.** The Venn diagram of overlapping and nonoverlapping unique phosphopeptides found in all three phosphopeptides enrichment workflows. The drawing is not proportionate.

However, the ERLIC approach has the advantage of being a single, and not a two-step process, resulting in significantly higher sample recovery. More than 65% of samples loss was noted when SCX fractions were subjected to IMAC enrichment in SCX-IMAC workflow as compared to SCX-only workflow (Table 1). However, part of this loss may be due to loss of the nonphosphopeptide species. We also noted that there was a >50% increase in number of peptides recovered by WAX chromatography versus SCX chromatography suggesting that WAX column has a higher binding efficiency due possibly to the many acidophilic peptide species that in turn might cause a high level of peptide redundancy observed in ERLIC method. We calculated the number of D (Asp) and E (Glu) residues per phosphopeptide hit; the number of D/E per phosphopeptide in ERLIC is much higher than SCX-IMAC and SCX-only approaches. On average, 3.7 D and 4.2 E per phosphopeptide were observed in ERLIC workflow, whereas 1.7 D and 2.3 E residues per phosphopeptide were found in SCX-IMAC workflow. For SCX-only workflow, 1.6 D and 1.9 E per phosphopeptide were observed. This suggested ERLIC tends to bind more acidic phosphopeptides than typical tryptic peptides in general.

The single-step ERLIC method resulted in a 1-day reduction in process time (Table 1). Moreover, it has much higher efficiency and quality in phosphopeptide enrichment than SCX-only method. Nonetheless, the ERLIC method needs further improvement, particularly in reducing the redundancies. Although the enrichment is high, the high redundancies imply the separation and fractionation efficiency is low, resulting in high-abundance phosphopeptides distributed in multiple fractions. Enhancing the column separation efficiency may reduce the redundancies and significantly increase the number of unique phosphopeptides.[29]

**Phosphopeptides Distribution.** Together, the three methods identified a total of 2058 unique phosphopeptides, of which 1801 (88%) were identified by only one of the methods (Figure 2). Of these 1801 phosphopeptides, SCX-IMAC accounted for 57%, ERLIC for 38% and SCX-only for 5% (Figure 2). When the

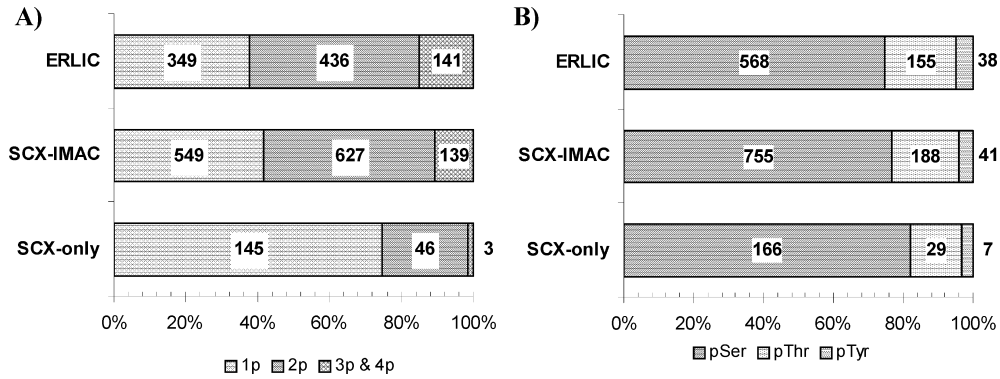


**Figure 3.** The distribution profile of unique phosphopeptides based on the number of phosphorylation sites (A) and phosphorylated amino acid residue (B) according to the different workflows.

SCX-only approach was not considered, the overlapping phosphopeptides identified by both SCX-IMAC and ERLIC approaches was 12% (data not shown). This observation was in accordance with a previous study comparing different methods (IMAC and $TiO_2$, or IMAC and PAC, or PAC and $TiO_2$) where only one-third of overlapping phosphorylation sites were noticed.[15]

Without phosphopeptide enrichment, most (75%) unique phosphopeptides identified by SCX were singly phosphorylated (Figure 3A). When coupled with IMAC, 58% of the unique phosphopeptides identified were doubly, triply, or quadruply phosphorylated with the singly phosphorylated reduced to 42% (from 75% in SCX-only approach). Anecdotal observations among IMAC users have suggested that IMAC binds only about 10−30% of a monophosphopeptide but 70−100% of peptides with two or more phosphates if the phosphopeptide-binding capacity of the IMAC resin is limiting. For example, when Zhang et al. performed two successive IMAC enrichment steps on the same sample, they observed that the first enrichment step yielded primarily diphosphopeptides, with monophosphopeptides constituting about 30% of the total, while the second IMAC step yielded almost exclusively monophosphopeptides.[30] This could explain why 75% of the unique phosphopeptides identified here by SCX-only workflow were singly phosphorylated, while only 42% were singly phosphorylated in the SCX-IMAC workflow. In the ERLIC method, 38% of the unique phosphopeptides were singly phosphorylated and 62% have ≥2 phosphorylated sites (Figure 3A). This is not unexpected as the positively charged WAX column binds peptides with higher numbers of negatively charged phosphate group more efficiently and will therefore tend to enrich for phosphopeptides with ≥2 phosphorylated sites over the monophosphopeptides.

The distribution of phosphorylated amino acid residues on the unique phosphopeptides was similar across all three methods with most phosphorylation occurring at Ser followed by Thr and then Tyr (Figure 3B), consistent with most reported observations.[7,14] Among total phosphorylation sites, the distribution of pSer, pThr, and pTyr in SCX-only and SCX-IMAC was 88%, 10%, and 2%, respectively, while that in the ERLIC workflow was 93%, 6%, and 1%, respectively (data not shown). However if the distribution of phosphorylated amino acid residues was considered on unique phosphopeptides only in SCX-only, SCX-IMAC and ERLIC (Figure 3B), pSer decreased, respectively, to 82.2%, 76.7%, and 74.6%, pThr increased slightly to 14%, 19%, and 20%, while pTyr increased to 3.5%, 4.2%, and 5.0%. Therefore, by eliminating the redundancy and considering only unique phosphopeptides, the distribution profile of phosphorylated amino acid was more similar between ERLIC and SCX-IMAC than that between SCX-IMAC and SCX-only. The increase in pTyr upon reducing redundancy in all three methods of enrichment implies that pTyr residues tend to be on phosphopeptides of lower abundance, and most literatures reported pTyr residues to constitute 1−2%.[7,31] The more substantial increase from 1 to 5% in the ERLIC method also suggests that ERLIC identifies more phosphopeptides of lower abundance.

At pH 2.0 (for ERLIC condition) or pH 2.65 (for SCX condition), D and E would be substantially uncharged. Therefore, in order to estimate the net solution charge state, we assumed every ionizable residue to be fully uncharged, except those residues carrying a phosphate group. By calculation, each phosphate group contributes a charge state value of −1 to the overall peptide solution charge state.[14] The net solution charge state was calculated based on the observed peptide charge (deduced from MASCOT) minus number of phosphorylation sites[14] (Figure 4). The two chromatographic separations operate in an opposite manner, with one cation-based and the other anion-based. For SCX-IMAC, the net solution charge state rises from 0 to 2.2 as the fraction number increases, while the net solution charge decreases from 2.0 to −1.1 for a WAX column (i.e., ERLIC) (Figure 4). The number of phosphopeptides identified in each fraction from both workflows was well-distributed. The exception was noted during the first 3 fractions in ERLIC (Figure 4). These first 3 fractions corresponded to the ERLIC flow through, which indicated the higher charge peptides did not bind to the column, and these peptides are typically nonphosphorylated. This observation suggests that the majority of the phosphopeptides are successfully captured under the ERLIC mode in a WAX column with a remarkably high binding efficiency. In contrast, the SCX separation serves only to separate the complex peptide mixture into a simpler content such that the next IMAC step could target a smaller set of sample for higher phosphopeptides enrichment efficiency. Since phosphopeptides carry negative charges (−), based on the principle of ERLIC, phosphopeptides with 2 or more phosphate groups will tend to bind stronger to the WAX column.

**Motif Analysis.** To understand the phosphopeptide motifs identified by SCX-IMAC and ERLIC methods, the phosphoproteome data sets were analyzed by the Motif-X algorithm.[22] The smaller data set from SCX-only was excluded in this analysis due to a lack of motif representation. We have identified 21 and 17 motifs using data sets from SCX-IMAC and ERLIC respectively. Approximately one-third of them are found repeatedly in both

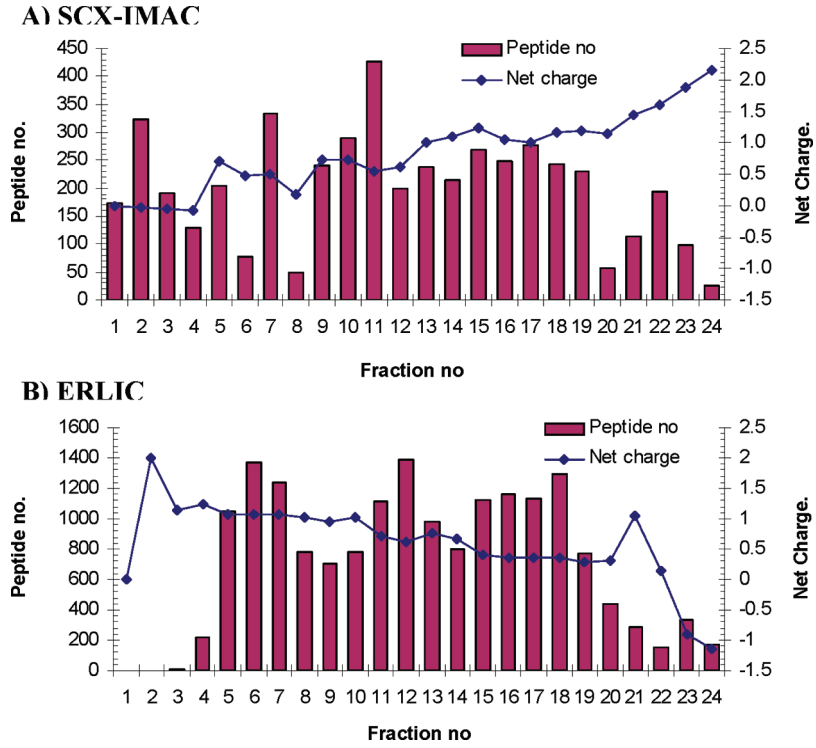


**Figure 4.** The bar chart indicated the number of phosphopeptides in each fraction, whereas the line chart showed the average peptide (net) charge state at pH 2.65 and pH 2.00 for (A) SCX-IMAC workflow and (B) ERLIC workflow, respectively. The net charge was calculated based on the observed peptide charge minus number of phosphorylation sites, with each phosphorylation site of −1 charge.[14]

approaches, especially Casein Kinase II (CK2) substrate motif such as sDxExE and sDEEx (see Supporting Information Table S3). Similar observations were reported elsewhere with CK2 like motifs being the dominant feature in their data sets.[14,27,32] There were also many acidophilic motifs rich in D and E residues that are highly homologous to the CK2 like motif (see Supporting Information Table S3).

ERLIC method had a better coverage of acidophilic motifs (65%) as compared to SCX-IMAC (52%), while SCX-IMAC has a better coverage of basophilic motifs (14%) versus none detected by the ERLIC method (see Supporting Information Table S3). Proline-directed motifs were well-represented in both workflows with 33% and 18% for SCX-IMAC and ERLIC, respectively. These findings were in accordance with the reported principle of ERLIC where negatively charged peptides should have a higher binding efficiency toward a WAX column such as D and E containing peptides/phosphopeptides.

Consistent with these observations, the average negative peptide charge state based on the number of phosphorylation sites and the frequency of D and E residues in the peptide sequence was calculated to be −4.7 for the SCX-only method, which retains most of the basic peptides, IMAC enrichment through metal affinity interactions enhanced selection for the negatively charged peptides and decreased the average peptide charge state from −4.7 to −5.8. The ERLIC method was even more selective for negatively charged peptides and the average peptide charge state decreased more steeply, from −4.7 to −9.4.

**Proteins Interaction Network.** The above discussion prompts us to combine results generated from several complementary phosphopeptide enrichment methods to get a more complete phosphoproteome. The combination of ERLIC, SCX-IMAC and SCX-only approaches identified 768 unique phosphoproteins out of a total of 2561 proteins (Table 1). Not unexpectedly, the SCX-IMAC workflow identified the largest number of phosphoproteins at 520 followed by ERLIC at 365 proteins. In spite of low phosphopeptides enrichment, SCX-only identified 127 phosphoproteins (Table 1). The unique phosphoproteins from all three data sets were combined and analyzed using NetworKIN,[2] and Cytoscope,[24] a protein interaction network analysis software (Figure 5). Nonphosphorylated proteins were also included in NetworKIN network.

There are 317 known EGFR substrates (as reported in NetworKIN), of which 68 were represented in our data sets with 32 of them being in a phosphorylated state (Figure 5). Of the 4 known kinase substrates in the EGFR network, the cAMP-dependent protein kinase, alpha-catalytic subunit (PRKCA), was the only one that was positively identified as phosphorylated in this study. PRKCA in turn was known to have an amazing 1116 substrates (as reported in NetworKIN) and its substrate motif, identified in this study, was a basophilic motif known as Protein Kinase A/Protein Kinase C (PKA/PKC) substrate motif (Supporting Information Table S3). Of these 1116 PRKCA substrates, we were able to identify 277, with 186 in a phosphorylated state.

When comparing the 32 phosphorylated EGFR substrate proteins (Figure 5), it is clear that none of the phosphopeptides extraction methods used here could identify all of them. The SCX-IMAC, ERLIC and SCX-only workflow identified 22, 21, and 9, respectively. Not surprisingly, the SCX-only workflow did not yield any unique phosphorylated proteins due to its low resolving power during phosphopeptides separations. On the other hand, out of 32 phosphorylated proteins, 9 were unique to the SCX-IMAC workflow, whereas 10 were identified exclusively via the ERLIC workflow. This observation once again emphasizes the importance of using more than 1 extraction workflow for better phosphoprotein coverage, and more im-

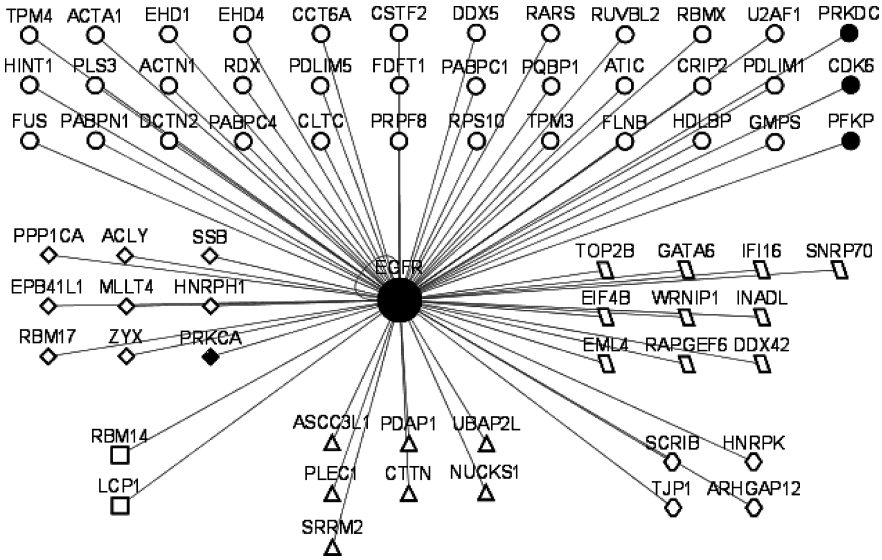


**Figure 5.** EGFR protein substrate interaction network. Nonphosphorylated proteins are in round shape (○), whereas phosphorylated proteins identified in different workflows are in other shapes. Parallelogram (▱), ERLIC; diamond (◇), SCX-IMAC; hexagon (⬡), ERLIC and SCX-IMAC; triangle (△), ERLIC, SCX-IMAC, and SCX-only; square (□), SCX-IMAC and SCX-only. Kinases are filled with black. The information about protein kinases are retrieved from NetworKIN.[2]

portantly, these two workflows, SCX-IMAC and ERLIC, complement each other well.

Among the unique proteins identified in SCX-IMAC workflow is ATP-citrate synthase (ACLY) which has 5 known phosphorylated sites. We have specifically identified the S455 site (verified by $MS^3$ scan) that is known to be regulated by PKA kinase. Another unique protein is isoform 4 of Avadin (MLLT4) which was found to be phosphorylated at site S1173 and S1182 with both sites verified by $MS^3$ scan. MILLT4 participates in the assembly and adhesion activity of E-cadherin which is essential for cell adhesion.[33] Interestingly these two sites (S1173 and S1182) have not been reported. These two examples show that the unique phosphopeptides identified in the SCX-IMAC workflow can have both low and high numbers of D/E residues in the peptides. For MLLT4, only 1 D/E residue was detected, whereas for ACLY, 3 D/E residues were observed.

One of the known EGFR substrates, Isoform Beta-2 of DNA topoisomerase (TOP2B), has 17 known phosphorylation sites. Two of the phosphorylation sites, S1522 and S1524, were present only in our ERLIC data set and were verified with a $MS^3$ scan (Figure 5). These sites are known to be phosphorylated by CKII kinase and carry the acidophilic motif sDxDxE. This supports our finding that the ERLIC method enriches for acidophilic phosphopeptides. Echinoderm microtubule-associated protein-like 4 (EML4) was the other known EGFR substrates that was only identified in the ERLIC method (Figure 5). It has 5 known phosphorylated sites and of these, T899 which is known to be phosphorylated by GSK3 or CDK5, has MASCOT peptide score of 62 and expectation value of $2 \times 10^{-4}$, but did not have an $MS^3$ scan. We also found that T897 was phosphorylated (after manual validation) and phosphorylation at this site has not been reported, suggesting that ERLIC is a valuable novel phosphopeptide enrichment technique that complements existing methods for discovery of new phosphorylation sites.

## Conclusion

This study which aimed to compare the ERLIC and SCX-IMAC approaches in enriching for phosphopeptides for MS-based identification demonstrated that, like other approaches for enriching phosphopeptides, the ERLIC and SCX-IMAC approaches are, by themselves, not comprehensive in their coverage of all the phosphopeptides in a given proteome.[15,27] Although the distribution of pSer, pThr and pTyr is similar for both approaches, the ERLIC approach identified a higher number of di- and triphosphopeptides efficiently than the SCX-IMAC approach. The low 12% overlap in unique phosphopeptides identified using the ERLIC or SCX-IMAC approach indicates that these two approaches identified overlapping but different subsets of phosphopeptides. This can be attributed primarily to diametrically opposite parameters underlying the enrichment process used in the one-step ERLIC approach or two-step SCX-IMAC approach. Enrichment for phosphopeptides was based on the electrostatic attraction between negatively charged phosphopeptides and the WAX column, and the electrostatic repulsion between nonphosphopeptides and the WAX column. In the SCX-IMAC approach, selective elution of negatively charged phosphopeptides by electrostatic repulsion in SCX column is followed by phosphopeptides enrichment using IMAC. Consequently, the ERLIC approach whose efficiency for enriching phosphopeptides is directly proportional to the negative charges on the peptides identified more phosphopeptides with $\geq 2$ phosphorylation sites. Therefore, it identified more phosphorylation sites even though the number of unique phosphopeptides identified is less than that identified by SCX-IMAC approach. It is also more efficient at identifying less abundant phosphopeptides and provides better coverage of phosphopeptides with acidophilic motifs.

On the other hand, the SCX-IMAC approach enriched for more phosphopeptides, albeit those with 1 phosphorylation site. Although the total number of phosphopeptides identified is lower, there is also lower redundancy with more unique phosphopeptides being identified. Unlike the ERLIC approach, its coverage includes peptides with both basophilic and acidophilic motifs.

Operationally, the ERLIC approach offers several advantages over the SCX-IMAC approach. One, it is a single-step chromatography method with the potential of being incorporated into

high-throughput automated processes. Being a newly developed method, it still has much room for optimization that might greatly improve its coverage of phosphorylation sites in a proteome. For example, the significant number of charged D and E containing phosphopeptides observed in the ERLIC approach here could be neutralized by the use of methanolic HCl.[34] Alternatively, a stronger buffer solution relative to the 10 mM Na-MePO$_4$ used in the Solvent A (ERLIC approach) may lead to a more thorough uncharging of carboxyl-groups. The present inferiority of the ERLIC approach relative to the better-established SCX-IMAC approach in detecting unique phosphopeptides can be further optimized. For example, the nonvolatile salt (TEAP) gradient for elution of peptides from the WAX column could be replaced with a more volatile salt such as ammonium formate/acetate/chloride as an alternative.[29] However, these modifications or optimizations are unlikely to extend the ERLIC's coverage of phosphopeptides to include those covered by the SCX-IMAC approach, for example, the phosphopeptides with basophilic motifs.

In conclusion, our study demonstrates that SCX-IMAC and ERLIC approaches exploit different strategies for the enrichment of different subsets of phosphopeptides that share some overlap. Therefore, these approaches should be used in complementation to enrich for a more diverse group of phosphopeptides to obtain a more comprehensive coverage of the phosphoproteome.

**Data Availability.** The database search result of MS$^2$ and MS$^3$ spectra in MASCOT Peptide View format is available via Internet at http://proteomics.sbs.ntu.edu.sg/~ERLIC_SCX-IMAC/MascotPeptideView.html

**Abbreviations:** ERLIC, electrostatic repulsion-hydrophilic interaction chromatography; IMAC, immobilized metal affinity chromatography; SCX, strong cation exchange; WAX, weak anion exchange; FP, false positives; MS$^2$, 2 stages mass spectrometric analyses (MS/MS); MS$^3$, 3 stages mass spectrometric analyses (MS/MS/MS).

**Acknowledgment.** We express our gratitude to Andrew Alpert of PolyLC, Inc. for his critical advice and timeless hours of technical support. We also thank Dominique de Kleijn for invaluable discussion. Tiannan Guo is supported by a grant from the National Cancer Centre Singapore Research Foundation. This work is supported by grants from Biomedical Research Council (BMRC: 07/1/22/19/531) and Ministry of Education (ARC: T206B3211) of Singapore.

**Supporting Information Available:** The complete list of phosphopeptides identified in SCX-only, SCX-IMAC and ERLIC (Supplementary Table S1). The MS$^3$ identification for all three workflows (Supplementary Table S2). General motif classes for all workflows (Supplementary Table S3). Panther protein classification for molecular function and biological processes (Supplementary Figure S1). This material is available free of charge via the Internet at http://pubs.acs.org.

## References

(1) Hubbard, M. J.; Cohen, P. On target with a new mechanism for the regulation of protein phosphorylation. *Trends Biochem. Sci.* **1993**, *18* (5), 172–7.
(2) Linding, R.; Jensen, L. J.; Pasculescu, A.; Olhovsky, M.; Colwill, K.; Bork, P.; Yaffe, M. B.; Pawson, T. NetworKIN: a resource for exploring cellular phosphorylation networks. *Nucleic Acids Res.* **2008**, *36* (Database issue), D695−9.
(3) Amanchy, R.; Periaswamy, B.; Mathivanan, S.; Reddy, R.; Tattikota, S. G.; Pandey, A. A curated compendium of phosphorylation motifs. *Nat. Biotechnol.* **2007**, *25* (3), 285–6.
(4) Gnad, F.; Ren, S.; Cox, J.; Olsen, J. V.; Macek, B.; Oroshi, M.; Mann, M. PHOSIDA (phosphorylation site database): management, structural and evolutionary investigation, and prediction of phosphosites. *Genome Biol.* **2007**, *8* (11), R250.
(5) Smith, J. C.; Figeys, D. Recent developments in mass spectrometry-based quantitative phosphoproteomics. *Biochem. Cell. Biol.* **2008**, *86* (2), 137–48.
(6) Yarden, Y.; Shilo, B. Z. SnapShot: EGFR signaling pathway. *Cell* **2007**, *131* (5), 1018.
(7) Olsen, J. V.; Blagoev, B.; Gnad, F.; Macek, B.; Kumar, C.; Mortensen, P.; Mann, M. Global, in vivo, and site-specific phosphorylation dynamics in signaling networks. *Cell* **2006**, *127* (3), 635–48.
(8) Johns, T. G.; Perera, R. M.; Vernes, S. C.; Vitali, A. A.; Cao, D. X.; Cavenee, W. K.; Scott, A. M.; Furnari, F. B. The efficacy of epidermal growth factor receptor-specific antibodies against glioma xenografts is influenced by receptor levels, activation status, and heterodimerization. *Clin. Cancer Res.* **2007**, *13* (6), 1911–25.
(9) Tao, W. A.; Wollscheid, B.; O'Brien, R.; Eng, J. K.; Li, X. J.; Bodenmiller, B.; Watts, J. D.; Hood, L.; Aebersold, R. Quantitative phosphoproteome analysis using a dendrimer conjugation chemistry and tandem mass spectrometry. *Nat. Methods* **2005**, *2* (8), 591–8.
(10) Rush, J.; Moritz, A.; Lee, K. A.; Guo, A.; Goss, V. L.; Spek, E. J.; Zhang, H.; Zha, X. M.; Polakiewicz, R. D.; Comb, M. J. Immunoaffinity profiling of tyrosine phosphorylation in cancer cells. *Nat. Biotechnol.* **2005**, *23* (1), 94–101.
(11) Ficarro, S. B.; McCleland, M. L.; Stukenberg, P. T.; Burke, D. J.; Ross, M. M.; Shabanowitz, J.; Hunt, D. F.; White, F. M. Phosphoproteome analysis by mass spectrometry and its application to Saccharomyces cerevisiae. *Nat. Biotechnol.* **2002**, *20* (3), 301–5.
(12) Beausoleil, S. A.; Jedrychowski, M.; Schwartz, D.; Elias, J. E.; Villen, J.; Li, J.; Cohn, M. A.; Cantley, L. C.; Gygi, S. P. Large-scale characterization of HeLa cell nuclear phosphoproteins. *Proc. Natl. Acad. Sci. U.S.A.* **2004**, *101* (33), 12130–5.
(13) Larsen, M. R.; Thingholm, T. E.; Jensen, O. N.; Roepstorff, P.; Jorgensen, T. J. Highly selective enrichment of phosphorylated peptides from peptide mixtures using titanium dioxide microcolumns. *Mol. Cell. Proteomics* **2005**, *4* (7), 873–86.
(14) Villen, J.; Beausoleil, S. A.; Gerber, S. A.; Gygi, S. P. Large-scale phosphorylation analysis of mouse liver. *Proc. Natl. Acad. Sci. U.S.A.* **2007**, *104* (5), 1488–93.
(15) Bodenmiller, B.; Mueller, L. N.; Mueller, M.; Domon, B.; Aebersold, R. Reproducible isolation of distinct, overlapping segments of the phosphoproteome. *Nat. Methods* **2007**, *4* (3), 231–7.
(16) Gruhler, A.; Olsen, J. V.; Mohammed, S.; Mortensen, P.; Faergeman, N. J.; Mann, M.; Jensen, O. N. Quantitative phosphoproteomics applied to the yeast pheromone signaling pathway. *Mol. Cell. Proteomics* **2005**, *4* (3), 310–27.
(17) Zhang, Y.; Wolf-Yadlin, A.; Ross, P. L.; Pappin, D. J.; Rush, J.; Lauffenburger, D. A.; White, F. M. Time-resolved mass spectrometry of tyrosine phosphorylation sites in the epidermal growth factor receptor signaling network reveals dynamic modules. *Mol. Cell. Proteomics* **2005**, *4* (9), 1240–50.
(18) Alpert, A. J. Electrostatic repulsion hydrophilic interaction chromatography for isocratic separation of charged solutes and selective isolation of phosphopeptides. *Anal. Chem.* **2008**, *80* (1), 62–76.
(19) Sze, S. K.; de Kleijn, D. P.; Lai, R. C.; Khia Way Tan, E.; Zhao, H.; Yeo, K. S.; Low, T. Y.; Lian, Q.; Lee, C. N.; Mitchell, W.; El Oakley, R. M.; Lim, S. K. Elucidating the secretion proteome of human embryonic stem cell-derived mesenchymal stem cells. *Mol. Cell. Proteomics* **2007**, *6* (10), 1680–9.
(20) Kersey, P. J.; Duarte, J.; Williams, A.; Karavidopoulou, Y.; Birney, E.; Apweiler, R. The International Protein Index: an integrated database for proteomics experiments. *Proteomics* **2004**, *4* (7), 1985–8.
(21) Elias, J. E.; Gygi, S. P. Target-decoy search strategy for increased confidence in large-scale protein identifications by mass spectrometry. *Nat. Methods* **2007**, *4* (3), 207–14.
(22) Schwartz, D.; Gygi, S. P. An iterative statistical approach to the identification of protein phosphorylation motifs from large-scale data sets. *Nat. Biotechnol.* **2005**, *23* (11), 1391–8.
(23) Mi, H.; Lazareva-Ulitsky, B.; Loo, R.; Kejariwal, A.; Vandergriff, J.; Rabkin, S.; Guo, N.; Muruganujan, A.; Doremieux, O.; Campbell, M. J.; Kitano, H.; Thomas, P. D. The PANTHER database of protein families, subfamilies, functions and pathways. *Nucleic Acids Res.* **2005**, *33* (Database issue), D284−8.

(24) Shannon, P.; Markiel, A.; Ozier, O.; Baliga, N. S.; Wang, J. T.; Ramage, D.; Amin, N.; Schwikowski, B.; Ideker, T. Cytoscape: a software environment for integrated models of biomolecular interaction networks. *Genome Res.* **2003**, *13* (11), 2498–504.
(25) Ulintz, P. J.; Bodenmiller, B.; rews, P. C.; Aebersold, R.; Nesvizhskii, A. I. Investigating MS2/MS3 matching statistics: a model for coupling consecutive stage mass spectrometry data for increased peptide identification confidence. *Mol. Cell. Proteomics* **2008**, *7* (1), 71–87.
(26) Beausoleil, S. A.; Villen, J.; Gerber, S. A.; Rush, J.; Gygi, S. P. A probability-based approach for high-throughput protein phosphorylation analysis and site localization. *Nat. Biotechnol.* **2006**, *24* (10), 1285–92.
(27) Wilson-Grady, J. T.; Villen, J.; Gygi, S. P. Phosphoproteome analysis of fission yeast. *J. Proteome Res.* **2008**, *7* (3), 1088–97.
(28) Smith, J. C.; Duchesne, M. A.; Tozzi, P.; Ethier, M.; Figeys, D. A differential phosphoproteomic analysis of retinoic acid-treated P19 cells. *J. Proteome Res.* **2007**, *6* (8), 3174–86.
(29) Alpert, A.; Mitulović, G.; Mechtler, K. Isolation of Tryptic Phosphopeptides by ERLIC (Electrostatic Repulsion-Hydrophilic Interaction Chromatography) ABRF Conference, 2008, poster P31-S.
(30) Zhang, X.; Ye, J.; Jensen, O. N.; Roepstorff, P. Highly efficient phosphopeptide enrichment by calcium phosphate precipitation combined with subsequent IMAC enrichment. *Mol. Cell. Proteomics* **2007**, *6* (11), 2032–42.
(31) Hunter, T.; Sefton, B. M. Transforming gene product of Rous sarcoma virus phosphorylates tyrosine. *Proc. Natl. Acad. Sci. U.S.A.* **1980**, *77* (3), 1311–5.
(32) Li, X.; Gerber, S. A.; Rudner, A. D.; Beausoleil, S. A.; Haas, W.; Villen, J.; Elias, J. E.; Gygi, S. P. Large-scale phosphorylation analysis of alpha-factor-arrested Saccharomyces cerevisiae. *J. Proteome Res.* **2007**, *6* (3), 1190–7.
(33) Sato, T.; Fujita, N.; Yamada, A.; Ooshio, T.; Okamoto, R.; Irie, K.; Takai, Y. Regulation of the assembly and adhesion activity of E-cadherin by nectin and afadin for the formation of adherens junctions in Madin-Darby canine kidney cells. *J. Biol. Chem.* **2006**, *281* (8), 5288–99.
(34) Hunt, D. F.; Yates, J. R., 3rd; Shabanowitz, J.; Winston, S.; Hauer, C. R. Protein sequencing by tandem mass spectrometry. *Proc. Natl. Acad. Sci. U.S.A.* **1986**, *83* (17), 6233–7.

PR800473J